



HAL
open science

Large-scale flexuring and antithetic extensional faulting along a nascent plate boundary in the SE Afar rift

Bernard Le Gall, Mohamed Ahmed Daoud, Joël Rolet, Nima Moussa Egueh

► To cite this version:

Bernard Le Gall, Mohamed Ahmed Daoud, Joël Rolet, Nima Moussa Egueh. Large-scale flexuring and antithetic extensional faulting along a nascent plate boundary in the SE Afar rift. *Terra Nova*, 2011, 23 (6), pp.416-420. 10.1111/j.1365-3121.2011.01029.x . insu-00635012

HAL Id: insu-00635012

<https://insu.hal.science/insu-00635012>

Submitted on 26 Oct 2011

HAL is a multi-disciplinary open access archive for the deposit and dissemination of scientific research documents, whether they are published or not. The documents may come from teaching and research institutions in France or abroad, or from public or private research centers.

L'archive ouverte pluridisciplinaire **HAL**, est destinée au dépôt et à la diffusion de documents scientifiques de niveau recherche, publiés ou non, émanant des établissements d'enseignement et de recherche français ou étrangers, des laboratoires publics ou privés.

1 **LARGE-SCALE FLEXURING AND ANTITHETIC EXTENSIONAL FAULTING**
2 **ALONG A NASCENT PLATE BOUNDARY IN THE SE AFAR RIFT**

3
4 ***Bernard Le Gall¹, Mohamed Ahmed Daoud², Joel Rolet¹, and Nima Moussa Egueh^{1,2}**

5 ¹Université de Brest, CNRS; UMR 6538, IUEM, 29280 Plouzané, France.

6 ²Institut des Sciences de la Terre, Centre d'Etudes et de Recherches de Djibouti

7
8 *Corresponding author : 33 2 98 49 87 56, 33 2 98 49 87 60, blegall@univ-brest.fr

9
10 Short title : Structure of a nascent plate boundary in SE Afar

11
12 **ABSTRACT**

13 New structural data from the SE Afar margin in Djibouti leads us to discriminate two
14 recent (<1 Ma) extensional fault networks between the Afar accreted crust, and the South
15 Danakil Block to the east. Emphasis is placed on the N-S-oriented Makarassou fault system
16 which dissects the prominent westward- (riftward-)facing topographic flexure between the
17 two structural domains. The most striking characteristic of the Makarassou fault belt is a
18 closely-spaced network of continentward-dipping extensional faults, bounding domino blocks
19 of 3-1 Ma tilted lavas of the Stratoid series. The Makarassou fault-flexure system is
20 interpreted as an extensional faulted monocline that developed in response to differential
21 subsidence and crustal downwarping of the Afar magmatically-accreted transitional crust.
22 Large-scale flexuring and associated structures along the eastern flank of the Asal-Manda
23 Inakir incipient plate boundary are regarded as indicative of a nascent volcanic rifted margin
24 in SE Afar.

25
26 **Introduction**

27 Since the recognition of volcanic rifted margins (VRMs) in the 1980's (see Coffin and
28 Eldhom, 1994, for a review), the continent-ocean transition at VRMs is known to be
29 characterized by a typical style of crustal deformation and magmatic construction. Diagnostic
30 structures at VRMs comprise oceanward-thickening wedges of flood basalts displaying a
31 large-scale flexure, facing towards the ocean, and further dissected by a network of
32 continentward-dipping extensional faults (Mutter, 1984). The resulting seaward-dipping
33 reflector sequences (SDRS) pass laterally into oceanic crust (White and McKenzie, 1989).
34 Generally, the continent-ocean transition at VRMs is either partly under water, as along

35 modern ocean margins, or severely eroded within older exposed continental margins
36 (Klausen, 2009). Therefore, complete cross-strike transects of VRMs are rarely observed,
37 hence leading to uncertainties about, for example, the isostatic *versus* tectonic origin of the
38 overall fault-flexure pattern (Palmason, 1980; Nielsen and Brooks, 1981), or the timing and
39 duration of brittle strain with respect to the rifting and breakup events. These structural issues
40 are discussed here in the context of the SE Afar margin, where a magmatic fault-flexure
41 system is exceptionally exposed along the Asal active rift (Fig. 1) and interpreted as a
42 possible analog to a nascent VRM.

43

44 **SE Afar rift context**

45 The network of still-active tectono-magmatic axes that propagated since 3 Ma
46 throughout the Afar depression, ahead of the Red Sea and Aden oceanic ridges, form onshore
47 incipient plate boundaries between Arabia, Somalia and Nubia (Fig. 1B) (Mohr, 1989). In SE
48 Afar, the inland prolongation of the Aden ridge is outlined by the <1 Ma northerly-
49 propagating Ghoubbet-Asal and Manda-Inakir en echelon subrifts (Manighetti et al., 1998).
50 This modern rift axis cuts through the 3-1 Ma-old Stratoid flood basalts (Barberi and Varet,
51 1977) that cover most of the thin (18-22 km) and transitional crust of the Afar depression
52 (Dugda and Nyblade, 2006). The SE Afar magmatically-accreted domain is flanked to the
53 east by the South Danakil uplifted block *via* a prominent riftward-facing topographic scarp
54 representing the SE Afar margin (Fig. 1). The latter is further dissected by the N-S-trending
55 Makarassou fault system (MFS), which is generally regarded as a transfer zone linking the
56 Ghoubbet-Asal and Manda-Inakir subrifts (Tapponnier and Varet, 1974). Mechanisms of rift
57 propagation in SE Afar have been extensively discussed by Manighetti et al. (1998), but never
58 addressed in terms of uplift process. The role of vertical tectonics during the recent
59 development of the SE Afar margin is emphasized in the present work from the 3D-
60 morphostructural analysis of the Asal-South Danakil area.

61

62 **The South Danakil-Asal rift system**

63 Our structural study of the SE Afar margin is primarily based on 3D-morphostructural
64 data supplied by both Landsat ETM+ (resolution 15 m) and ASTER (60 x 60 km) satellite
65 images. ASTER digital elevation models (resolution 15 m) allow estimates of (1) fault and
66 lava dips, and (2) minimum vertical fault displacement from surface offsets along individual
67 fault scarps. Fault lengths, deduced from map traces, are underestimated because of the loss
68 of resolution below 15 m of vertical offset. Extensive field investigations did not permit the

69 observation of fault surfaces with slip criteria, because the lower parts of fault scarps are
70 systematically concealed by slope deposits, whereas their exposed upper sections usually
71 follow basaltic columnar jointing that rarely preserves the fault slip plane.
72 Field measurements were mostly devoted to calibrating fault and lava dips, estimated from
73 ASTER cross-profiles. The timing and magnitude of syn- to post-Stratoid regional uplift are
74 deduced from the spatial distribution, thickness variations and elevation of the Stratoid basalts
75 along the SE Afar margin.

76 The mapped extent of the Stratoid flood basalts on the western flank of the South
77 Danakil block suggests a two-stage uplift history which started in pre-Stratoid times with
78 initiation of the proto-Danakil block as a NE-plunging asymmetrical dome (Fig.
79 1A). Pronounced uplift is assumed to have continued in syn- to post-Stratoid times, in
80 combination with subsidence of the Afar accreted crust to the west. The resulting crustal-scale
81 downward bending occurred synchronously with the emplacement of the Stratoid basalts as a
82 volcanic wedge thickening westwards from a few 10's m on the Asa Gayla plateau, up to 100
83 m in the Makarassou fault belt, and > 1200 m in the Asal rift (Fig. 1C) (Zan et al., 1990).
84 Ongoing uplift of the proto-South Danakil block in post-Stratoid times caused the ~800 m
85 elevation of the initially horizontal Stratoid basalts towards the Day Mountains (Fig. 1A). The
86 onset of uplift might be as young as 125 kyr, by correlation with the Middle Pleistocene
87 conglomeratic fans that currently fringe the foot of the South Danakil range in the Tadjoura
88 coastal plain (Fig. 1B) (Gasse and Fournier, 1983).

89 During the last 3 Ma, the SE Afar margin recorded several episodes of extensional faulting in
90 various tectonic settings. The westernmost edge of the proto-South Danakil block (present-
91 day Asa Gayla plateau) developed as a >10 km-wide half-graben-like structure, filled with a
92 probably thin sequence of Stratoid basalts (S_2), and bounded to the east by an inferred
93 submeridian master fault (Fa on Figs. 1B and 1C). Uplift and erosion events in the footwall
94 block to the east are currently expressed by discrete inliers of deeply incised Lower Stratoid
95 basalts (S_1), resting horizontally on top of Dalha substratum volcanics. Two younger
96 extensional events finally led to the present-day fault arrangement along the SE Afar margin.
97 The <1 Ma Ghoubbet-Asal-Manda-Inakir en echelon subrift pattern along the subdued part of
98 the margin is not detailed here (see Manighetti et al., 1998). More interestingly for the present
99 issue is the structural development of the Makarassou fault system in the upper part of the SE
100 Afar topographic scarp.

101

102 **Structure of the Makarassou fault/flexure system**

103 The NS-trending structures of the Makarassou fault system extend through the western
104 flank of a prominent asymmetrical topographic range that culminates at 1800 m to the south,
105 in the Day Mountains, and slopes down, both northwards at 300 m in the Dorra plain, and
106 more abruptly westwards at <100 m in the Asal-Manda-Inakir rift floor (Fig. 1A). On the
107 Landsat ETM+ satellite image in Fig. 2A, the Makarassou fault system is a 70 km-long fault
108 belt that cuts the frontal part of the Stratoid basaltic wedge. It comprises two adjoining fault
109 subdomains, each 5 km wide, with contrasting structural styles. The high-density fault
110 subdomain to the east encloses a dense network of anastomosed and sigmoidal faults, about 5
111 km long on average. It is separated from the tabular Stratoid basalts of the Asa Gayla plateau
112 *via* the highly segmented fault Fb in Fig. 1C. Fault arrangement is more regular in the western
113 subdomain where four wider blocks are bounded by linear, and less segmented faults, >15 km
114 in length. There, the westerly-tilted Stratoid surfaces show remnants of NW-SE (Asal-type)
115 structures that are sharply cut, and thus post-dated, by the submeridian Makarassou bounding
116 faults (Fig. 2C). The northern termination of the Makarassou fault belt in the Dorra plain (Fig.
117 1B) is locally sealed by undeformed Manda Inakir basalts, >0.87 Ma in age (in Vellutini et al.,
118 1995).

119 The ~40 km-long transect in Fig. 1C cuts at high angle the widest exposed section of the
120 Makarassou fault system. Topography is dominated by a westerly-facing monoclinial flexure
121 that lowers the Stratoid surface to about 900 m, from the Asa Gayla plateau down to the Asal
122 rift floor. The hinge line of the Makarassou flexure approximately coincides with the NS-
123 trending trace of fault Fb (Fig. 2A). The two fault subdomains correspond to a
124 marked shallowing of topography westwards, with a flexure gradient decreasing from ~1°/km
125 to <0.5°/km. However, the most specific attribute of the Makarassou faults is the easterly
126 (outward) dip of 21 extensional structures (out of a total of 29). With the exception of
127 marginal horst-graben structures in the crestal zone to the east, the antithetic fault network
128 occurs strictly through the downflexed part of the cross-section (Fig. 1C). The resulting
129 inward-dipping Stratoid blocks are arranged in a domino configuration, with a mean spacing
130 of ~500 m, and rotated lava dips as high as 30°, in the upper and steepest part of the flexure
131 (Fig. 2B). Mean fault block width increases, up to 1 km, in the western subdomain,
132 concomitant with decreasing lava dips (10° in average). Average fault dip is about 70°E, and
133 remains nearly constant across-strike. Topographic fault scarps extracted from the ASTER 3D
134 models indicate vertical fault throws in the range 20-700 m, with a mean value of 105 m.

135

136 **Kinematic model and discussion**

137 From the new dataset above, the SE Afar margin is inferred to comprise two distinct
138 extensional fault networks that differ in terms of geometry, timing and kinematics. The Asal-
139 Manda-Inakir fault pattern bounds NW-SE-oriented en echelon horst/grabens, orthogonal to
140 the N30°E regional extension (e.g. Jestin et al., 1994), in the Afar depressed axis. In contrast,
141 the Makarassou extensional fault network is typically characterized by : (1) its spatial
142 association with a riftward-facing monoclinial flexure, (2) its outward-dipping attitude, away
143 from the rift axis, (3) its NS orientation, parallel to the flexure axis, and oblique to the
144 regional extension, and (4) its relatively young age with respect to the Asal structures.
145 Most of these structural features display striking similarities with those of coastal flexures
146 involving SDRS-type magmatic prisms along VRMs (Mutter, 1984). However, one specific
147 aspect of the Makarassou fault-flexure system is the lack of exposed mafic dyke swarms, but
148 these latter probably exist at depth, beneath the Stratoid fissural-type basalts.
149 These analogies lead us to evaluate whether the models applied to nascent VRMs could be
150 valid for the SE Afar volcano-tectonic pattern. Given the location of the Makarassou flexure
151 along the western edge of the Asa Gayla plateau, i.e. close to the hinge line marking the limit
152 of pronounced lava thickness towards the magmatically-accreted rift domain, we infer that
153 magma-assisted processes acted as driving forces for riftward-facing flexuring along the
154 western flank of the South Danakil block. By analogy with the isostatic model of Palmason
155 (1980), it is suggested that crustal downwarping along the SE Afar margin was the flexural
156 response to differential loading of the magmatically-accreted crust during the Stratoid (3-1
157 Ma), and even Dalha (8-4 Ma), flood basalt activity (Fig. 3C). Additional parameters are
158 thought to have interacted during flexuring, and to be responsible for the finite geometry of
159 the Makarassou fault-flexure system. Its NS orientation, oblique to the regional extension, is
160 believed to have followed preexisting structural fabrics. Indeed, the extensional rejuvenation
161 of inherited submeridian faults, such as those cutting the Mablás volcanics to the east, likely
162 accounts for the inferred syn-Stratoid bounding fault Fa (Figs. 1C and 3A). A steep and
163 similarly-trending weakness zone (Fb) is suspected to occur at depth, beneath the hinge line
164 of the flexure, further west. This resulted in an extensional monocline, analogous to those
165 developed above the upward-propagating tip of a blind normal fault (Willsey et al., 2002).
166 Dominantly dip-slip displacement, down to the west, and probably >500 m, likely occurred
167 along the steep discontinuity Fb, in order to accommodate part of the downflexed bending of
168 the Stratoid sequences at the surface. Assuming that the Makarassou flexure nucleated above

169 a steep weakness zone satisfactorily accounts for (1) its relative tightness (~10 km) with
170 respect to its total length, and (2) its concave profile, with higher flexure gradients in its upper
171 part.

172 The discontinuity Fb is believed to have once breached the monocline along a surface
173 breaking zone, currently outlined by the crestal horst-graben pattern. The network of
174 antithetic normal faults, splaying upwards into the immediate hangingwall of fault Fb,
175 resemble those directly observed, or obtained experimentally, in extensional monoclines
176 (Withjack et al., 1990; Kaven and Martel, 2007). But, their nucleation and development in the
177 downflexed Stratoid lava pile were probably controlled by volcanic structures, as follows.
178 Provided that the wedge-shaped pile of initially horizontal (Dalha-Stratoid) lava flows rotated
179 westwards, towards the axis of the active magmatic zone, during early flexuring, the cooling
180 joint pattern, known to generally act as tension fractures under tensile stress (Forslund and
181 Gudmundsson, 1992 ; Le Gall et al., 2000), likely evolved from an initially vertical attitude to
182 an easterly-inclined position with time (Fig. 3B). The decreasing dip attitude of the joint
183 pattern at depth resulted in a listric-shaped joint trajectory which might have later triggered
184 nucleation of normal faults, dipping away from the subsiding rift axis to the west, once
185 submitted to the N30°E-directed extension.

186 The isostatic, instead of tectonic, model proposed here for the Makarassou flexure is
187 reinforced by the fact that structural evidence are currently absent for a continentward-facing
188 detachment underlying the Stratoid wedge, as argued in the 'roll-over anticline' model
189 applied to SDRS prisms elsewhere (Geoffroy et al., 1998). Furthermore, the constant and
190 steeply-dipping attitude of extensional faults throughout the Makarassou flexure is at odds
191 with highly rotated hangingwall structures, typically developed above the frontal part of a
192 detachment (McKlay, 1996).

193 From the age of pre- (3-1 Ma) and post-flexuring (>0.87 Ma) basalts, the maximum duration
194 of the Makarassou flexure is ~2Ma, i.e. as similarly stated for others VRMs (Lenoir et al.,
195 2003 ; Klausen, 2009). Such a short time span suggests that regional strain rates were
196 relatively high during flexuring along the SE Afar margin, probably in relation with
197 anomalous thermal gradients at depth.

198 The magma-driven vertical tectonics and riftward-facing flexuring that operated during the
199 last 3 Ma, along the eastern flank of the Asal-Manda Inakir future plate boundary, are
200 confidently regarded as the structural expression of an incipient VRM in SE Afar. The inferred
201 embryonic stage of continental breakup is in agreement with previous assessments about the
202 transitional type of the Stratoid flood basalt series, and the thinned character of the Afar crust.

203

204 **Acknowledgments**

205 Funding and logistical support from CERD of Djibouti (Dir. Dr Mohamed Jalludin), and the
206 MAWARI program, are appreciated. Thanks also to the reviewers G. Eagles, A.
207 Gudmundsson and J. Rowland, and to the Associate Editor A. Nicolas for helpful and
208 constructive comments that improved a previous version of the manuscript. Stefan Lalonde is
209 warmly thanked for polishing the English.

210

211 **References cited**

212

213 Barbéri, F. and Varet, J., 1977. Volcanism of Afar :small-scale plate tectonics implications.
214 *Geol. Soc. Am. Bull.*, **88**, 1251-1266.

215 Coffin, M.F. and Eldhom, O., 1994. Large igneous provinces : Crustal structure, dimensions
216 and external consequences. *Rev. Geophys.*, **32**, 1-36.

217 Dugda, M.T. and Nyblade, A.A., 2006. New constraints on crustal structure in eastern Afar
218 from the analysis of receiver functions and surface waves dispersion in Djibouti. In :
219 *The Afar Volcanic Province Within The East African Rift System* (G. Yirgu, C.J.
220 Ebinger, P.K. Maguire, eds). *Geol. Soc. London, Sp. Pub.*, **259**, 239-251.

221 Forslund, T. and Gudmundsson, A., 1992. Structure of Tertiary and Pleistocene normal faults
222 in Iceland. *Tectonics*, **11**, 57-68.

223 Gasse, F. and Fournier, M., 1983. Sédiments plio-quaternaires et tectonique en bordure du
224 Golfe de Tadjoura, République de Djibouti. *Bull. Centres Recherche Exploration-
225 Production Elf-Aquitaine*, **7**, 285-300.

226 Geoffroy, L., Gélard, J.P., Lepvrier, C. and Olivier, P., 1998. The coastal flexure of Disko
227 (West Greenland), onshore expression of the ‘oblique reflectors’. *J. Geol. Soc. London*,
228 **155**, 463-473.

229 Jestin, F., Huchon, P. and Gaulier, J.M., 1994. The Somalia plate and the East African Rift
230 System : present kinematics. *Geophys. J. Intern.*, **116**, 637-654.

231 Kaven, J.O. and Martel, S.J., 2007. Growth of surface-breaching normal faults as a three-
232 dimensional fracturing process. *J. Struct. Geol.*, **29**, 1463-1476.

233 Klausen, B., 2009. The Lebombo monocline and associated feeder dyke swarm : Diagnostic
234 of a successful and highly volcanic rifted margin ? *Tectonophysics*, **468**, 42-62.

- 235 Le Gall, B., Le Turdu C., Richert J.P., Tiercelin J.J., Gente P., Sturchio P. and Stead, D.,
236 2000. A morphotectonic study of an extensional fault zone in a magma-rich rift type :
237 the Baringo Trachyte Fault System, Central Kenya Rift. *Tectonophysics*, **320**, 87-106.
- 238 Lenoir, X, Féraud, G. and Geoffroy, L., 2003. High-rate flexure of the East Greenland
239 volcanic margin : constraints from $^{40}\text{Ar}/^{39}\text{Ar}$ dating of basaltic dykes. *Earth and Planet.*
240 *Sc. Lett.*, **214**, 515-528.
- 241 Manighetti, I., Tapponnier, P., Gillot, P.Y., Jacques, E., Courtillot, V., Armijo, R., Ruegg,
242 J.C. and King, G., 1998. Propagation of rifting along the Arabia-Somalia plate
243 boundary : Into Afar. *J. Geophys. Research*, **103**, 4947-4974.
- 244 McKlay, K.R., 1996. Recent advances in analogue modelling : uses in section interpretation
245 and validation. In : *Modern Developments In Structural Interpretation, Validation And*
246 *Modelling*. (P.G. Buchanan and D.A. Nieuwland, eds.). *Geol. Soc. London, Sp. Pub.*,
247 **99**, 201-225.
- 248 Mohr, P., 1989. Nature of the crust under Afar : new igneous, not thinned continental :
249 *Tectonophysics*, **167**, 1-11.
- 250 Mutter, J.C., 1984. Seaward dipping reflectors and the continent-ocean boundary at passive
251 continental margins. *Tectonophysics*, **114**, 117-131.
- 252 Nielsen, T.F. and Brooks, C.K., 1981. The East-Greenland rifted continental margin : an
253 examination of the coastal flexure. *J. Geol. Soc., London*, **138**, 559-568.
- 254 Palmason, G., 1980. A continuum model of crustal generation in Iceland : Kinematics aspects.
255 *J. of Geophys.*, **47**, 7-18.
- 256 Tapponnier, P. and Varet, J., 1974. La zone de Mak'arrassou en Afar, un équivalent émergé
257 des failles transformantes océaniques. *C. R. Acad. Sc., Paris*, **274**, 209-212.
- 258 Vellutini, P., Piguët, P. and Recroix, F., 1995. Carte géologique de la République de Djibouti
259 au 1/100 000. Feuille de Dorra. In : *Notice explicative*. (BRGM, eds). Service
260 Géologique National, Orléans, 85 pp.
- 261 White, R.S. and McKenzie, D.P., 1989. Magmatism at rift zones : The generation of volcanic
262 continental margins and flood basalts. *J. Geophys. Res.*, **94**, 7685-7729.

- 263 Willsey, S.P., Umhoefer, P.J. and Hilley, G.E., 2002. Early evolution of an extensional
264 monocline by a propagating normal fault : 3D analysis from combined field study and
265 numerical modeling. *J. Struct. Geol.*, **24**, 651-669.
- 266 Withjack, M.O., Olson, J. and Peterson, E., 1990. Experimental models of extensional forced
267 folds. *Am. Assoc. Pet. Geol. Bull.*, **74**, 1038-1054.
- 268 Zan, L., Gianelli, P., Passerini, C., Troisi, A. and Haga, O., 1990. Geothermal exploration in
269 the Republic of Djibouti: thermal and geological data of the Hanlé and Asal areas.
270 *Geothermics*, **19**, 561-582.

271

272 **Figure captions**

273

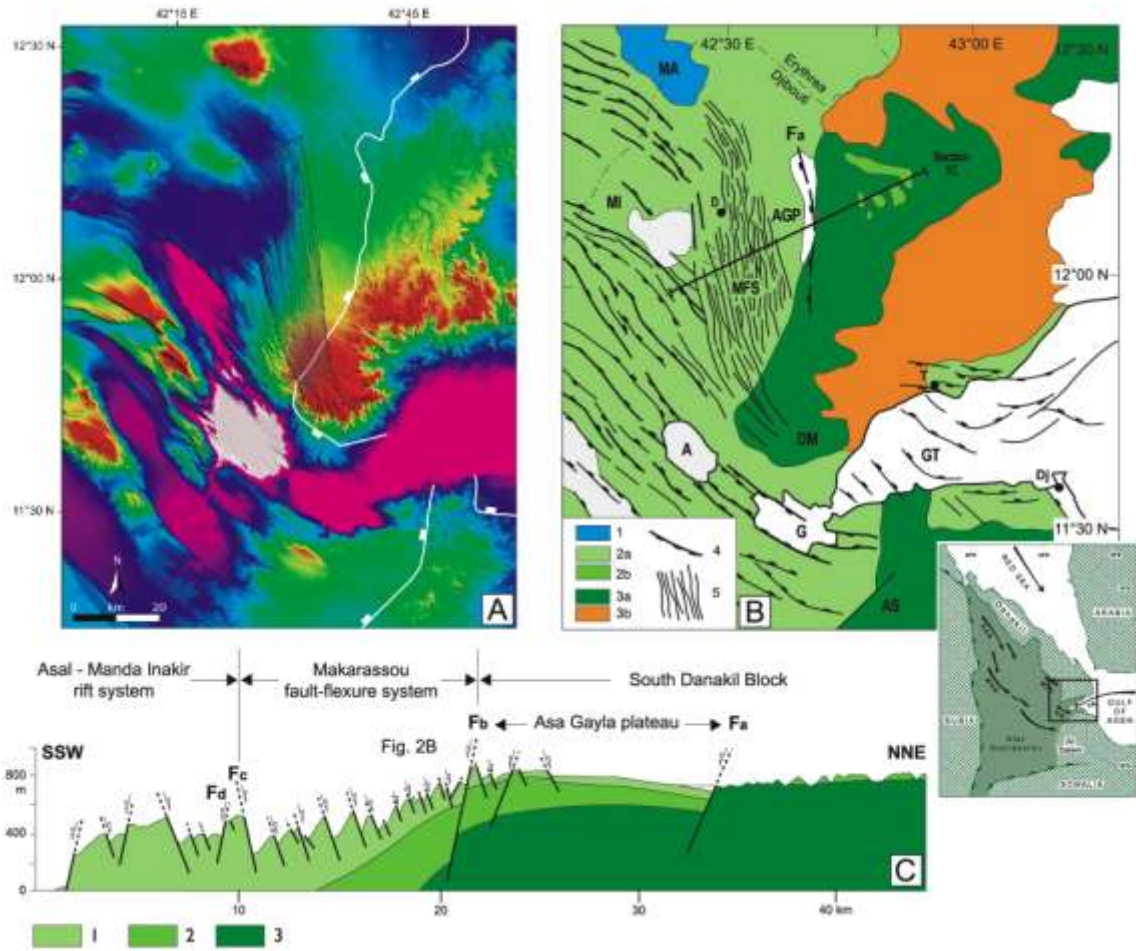
274 Fig. 1A. ASTER digital elevation model of the SE Afar rift in Djibouti (vertical resolution 15
275 m). Topography ranges from -150 m (Asal) up to 1800 m (Day Mountains). See
276 nomenclature in Fig. 1B. The white line shows the limit of Stratoid basalts (onshore).
277 Ticks are inside the volcanic area. Note its obliquity with respect to the South Danakil
278 reliefs. Fig. 1B. Structural sketch of the SE Afar margin in Djibouti. 1. Moussa Ali
279 volcanics ; 2a. 3-1 Ma Stratoid and Gulf basalts; 2b. Lower Stratoid basalts; 3. >3 Ma
280 synrift volcanics, 3a. Dalha basalts, 3b. Mablás Fm. ; 4. Main faults, 5. Makarassou
281 fault system. A., Asal ; AGP., Asa Gayla plateau ; AS., Ali Sabieh ; D., Dorra ; Dj.,
282 Djibouti ; DM., Day Mountains ; G., Ghoubbet ; GT., Gulf of Tadjoura ; MA., Moussa
283 Ali volcano ; MFS., Makarassou fault system ; MI., Manda Inakir; T., Tadjoura. Trace
284 of section 1C is drawn. Inset shows accretionary axes in the Afar Triple junction. 1C.
285 Structural cross-section of the central part of the Makarassou fault system. Topography
286 is extracted from the ASTER DEM. 1 and 2. S₁ and S₂ Stratoid basalts, respectively. 3.
287 Dalha basalts. Vertical exaggeration ~4. Location in Fig. 1B.

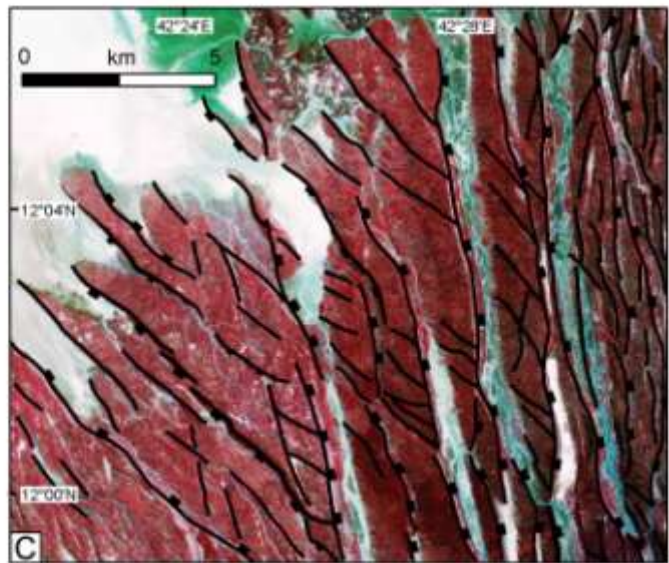
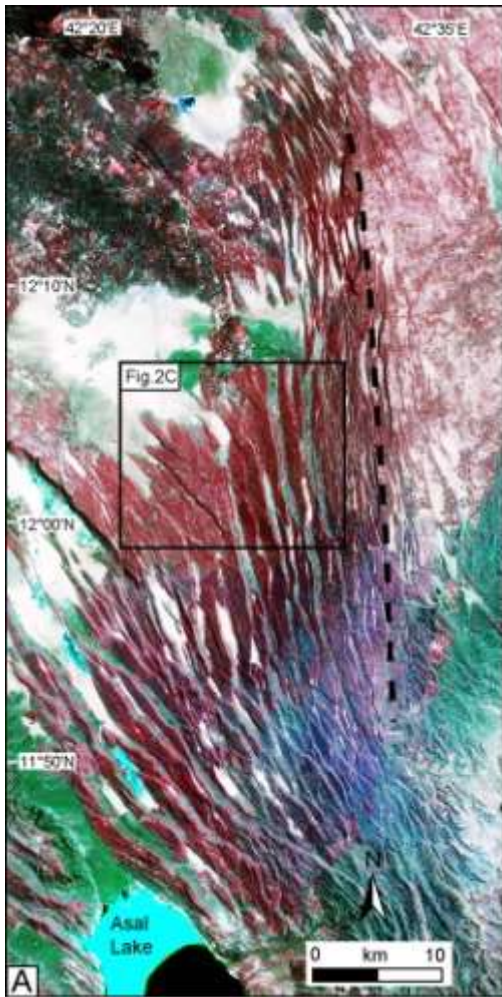
288

289 Fig. 2A. Map trace of the Makarassou fault belt on the eastern flank of the Asal-Manda Inakir
290 rift framework (Landsat ETM+ image, 15 m resolution). The dashed black line is the
291 trace of the flexure hinge line, close to the trace of fault Fb. 2B. Field view of a closely-
292 spaced network (~500 m) of three Stratoid tilted blocks (dip ~15°W), bounded by
293 easterly-facing extensional faults. View looking south. The main fault scarp in the back
294 is about 150 m high. Location in Fig. 1C. 2C. Focussed view of the Landsat ETM+
295 image (in Fig. 2A) showing Makarassou submeridian normal faults cutting NW-SE-
296 trending Asal horst-graben structures.

297
298
299
300
301
302
303
304
305
306
307
308
309
310
311
312
313
314
315
316

Fig. 3A. Sketch structural map of SE Afar emphasizing the role of inherited NS discontinuities on (1) the propagation of the Aden and Ghoubbet-Asal-Manda-Inakir incipient plate boundaries, and (2) initiation of the corresponding volcanic rifted margin (Makarassou belt). 1. <1 Ma rifted zones ; 2. Makarassou flexure ; 3. Onshore distribution of 3-1 Ma Stratoid and Gulf basalts; 4. Pre-Stratoid volcanics. A. Asal ; Ar. Arta ; G. Ghoubbet ; MFS. Makarassou fault system ; MI. Manda Inakir ; MT. Maskali transform. 3B. Conceptual model for the origin of outward-dipping extensional faults in wedges of flood basalts. 3C. Development of riftward-flexuring and antithetic extensional faulting along the SE Afar margin, as a consequence of magma-driven isostatic loading, and reactivated heterogeneities. 1. Stratoid basalts (3-1 Ma); 2. Dalha basalts (8-4 Ma); 3. Volcanic substratum (>8 Ma).

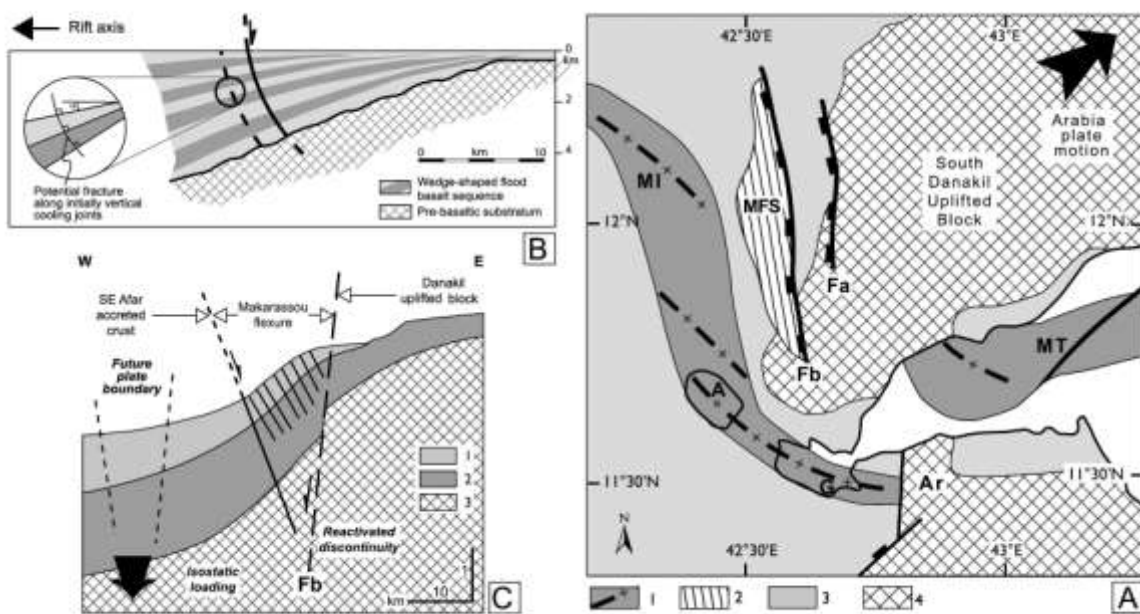




318

319

320



321